Geophysical Research Letters

RESEARCH LETTER
10.1029/2022GL098822

Key Points:

- Reanalysis data sets disagree on interannual variability and trends in moist static energy (MSE) transport
- Reanalysis MSE transport trends do not show a clear flux-gradient response to the MSE gradient trend
- Reanalysis MSE transport trends are dominated by fluxes of time-mean dry static energy by anomalous zonal mean meridional winds

Supporting Information:

Supporting Information may be found in the online version of this article.

Correspondence to:

J. P. Clark,
jc7377@princeton.edu

Citation:

Clark, J. P., Feldstein, S. B., & Lee, S. (2022). Moist static energy transport trends in four global reanalyses: Are they downgradient? *Geophysical Research Letters*, *49*, e2022GL098822. https://doi.org/10.1029/2022GL098822

Received 22 MAR 2022
Accepted 15 SEP 2022

Author Contributions:

Conceptualization: Joseph P. Clark
Formal analysis: Joseph P. Clark
Funding acquisition: Steven B. Feldstein, Sukyoung Lee
Methodology: Joseph P. Clark
Software: Joseph P. Clark
Supervision: Steven B. Feldstein, Sukyoung Lee
Visualization: Joseph P. Clark
Writing – original draft: Joseph P. Clark
Writing – review & editing: Steven B. Feldstein, Sukyoung Lee

Moist Static Energy Transport Trends in Four Global Reanalyses: Are They Downgradient?

Joseph P. Clark[1,2], Steven B. Feldstein[1], and Sukyoung Lee[1]

[1]Department of Meteorology and Atmospheric Science, The Pennsylvania State University, University Park, PA, USA, [2]Program in Atmospheric and Oceanic Sciences, Princeton University, Princeton, NJ, USA

Abstract Trends in moist static energy (MSE) transport are investigated for the years 1980 through 2018 using four different reanalysis data sets. The reanalysis data sets show agreement in the eddy MSE transport trends and the latitudinal structure of the MSE trends, but vary widely in the trend of the flux of the climatological zonal mean MSE by the anomalous zonal mean meridional wind. The latter dominates the total MSE transport trends in all four data sets. Therefore, none of the four total MSE flux trends is downgradient of the corresponding MSE trend. Further analysis of the MSE trends reveals that dry static energy increases strongly dominate MSE trends at all latitudes, including in the tropics where climate models and theory predict latent energy increases to dominate. As changes in MSE transport are routinely assumed to be downgradient when interpreting changes in climate, including Arctic amplification, further investigation of reanalysis MSE transport is warranted.

Plain Language Summary The Earth receives more energy than it loses over lower latitudes and loses more energy than it receives over high latitudes. Consistently, the atmospheric circulation fluxes much of the excess energy from low latitudes toward high latitudes where there is an energy deficit. This poleward movement of energy in the atmosphere plays a crucial role in shaping the climate, but it remains unclear how this energy transport will change as the climate warms. In this study, we investigate how energy transport has changed in recent decades using four different reanalysis data sets, data sets that obtain global coverage by combining atmospheric measurements with numerical models. We find that data sets do not agree on the trends in the energy transports which limits the extent to which they can be used to investigate energy transports. Nonetheless, reanalysis data sets do agree on certain aspects that contrast notably with climate models. First, energy transport trends in the reanalysis data sets do not flux energy from locations with high energy to locations with low energy. Second, reanalysis temperature increases drive greater increases in energy than that from water vapor, whereas in climate models water vapor increase is the most important contributor to the energy over the tropics.

1. Introduction

Moist static energy (MSE) is a useful thermodynamic variable for studying climate since this quantity is globally conserved in the absence of changes in energy fluxes at the top of the atmosphere and at the surface. Considering the important role that MSE transports play in shaping the climate (e.g., Hartmann, 2016; Peixoto & Oort, 1992), an ongoing research question that has been gaining attention is how MSE transports will change as the climate changes (Alexeev et al., 2005; Armour et al., 2019; Graversen & Wang, 2009; Held & Soden, 2006; Hwang & Frierson, 2010; Zelinka & Hartmann, 2012). In the time average, poleward transports of MSE reduce the energy surplus over the subtropics and tropics, where solar radiation exceeds terrestrial outgoing longwave radiation, and decrease the energy deficit over high latitudes, where terrestrial outgoing longwave radiation exceeds solar radiation (e.g., Carissimo et al., 1985; Hartmann, 2016; Peixoto & Oort, 1992). Poleward MSE transports thereby contribute to the maintenance of energy equilibrium at all latitudes.

The earliest climate modeling study on the effect that global warming has on MSE transports suggests an increase in poleward MSE transports in the tropics and a decrease in poleward MSE transports in the extratropics following the warming (Manabe & Wetherald, 1975; see their Figure 12a). However, more recent model studies have converged toward the conclusion that poleward MSE transports will increase at nearly all latitudes in response to warming (e.g., Held & Soden, 2006; Zelinka & Hartmann, 2012), with the exception of a narrow band centered near 70°N, where ensemble mean future projections suggest a small decrease in poleward MSE transports

accompanied by considerable spread, attributed to local feedbacks associated with Arctic amplification (Hwang et al., 2011).

Conceptually, poleward MSE transports are argued to increase with warming following Clausius-Clapeyron scaling (e.g., Armour et al., 2019; Held & Soden, 2006; Hwang & Frierson, 2010). For approximately the same increase in temperature and an approximately constant relative humidity, the greatest increase in water vapor will occur over locations with the highest climatological water vapor amounts—the tropical lower troposphere. It has been argued that a consequence of greater increases in water vapor over the tropics than the extratropics is a larger increase in MSE in the tropics compared to the extratropics and an enhanced poleward diffusion of MSE (Armour et al., 2019; Held & Soden, 2006; Hwang & Frierson, 2010). This argument is rooted also in an assumption that MSE transports act primarily to remove MSE gradients, that is, that MSE tranports obey a flux-gradient relationship.

Recent climate model projections support the notion that poleward MSE transports increase following warming. For example, the Coupled Model Intercomparison Project Phase 5 (CMIP5) ensemble mean simulates an increase in poleward MSE transports, accomplished by an increase in poleward dry static energy transport within the subtropics and an increase in poleward latent energy transport in the extratropics (Armour et al., 2019; Held & Soden, 2006). The model-simulated increase in dry static energy transport within the subtropics has been attributed to both an increase in the depth of the Hadley circulation and a reduction in the tropical lapse rate, leading to an increased dry static energy transport by the poleward branch of the Hadley circulation relative to that of the equatorward branch of the Hadley circulation (Held & Soden, 2006). In contrast, in the extratropics, the dominance of the latent energy contribution to the poleward MSE transport trend (Armour et al., 2019; Held & Soden, 2006) has been tied more directly to the increase in moisture following the constant relative humidity assumption and an assumption that circulation changes are negligible.

Apart from the relevance that MSE transports have on the spatial pattern of precipitation trends (e.g., Held & Soden, 2006), MSE transports are also relevant for the spatial distribution of temperature trends (Alexeev et al., 2005; Armour et al., 2019; Graversen & Wang, 2009; Hwang et al., 2011; Hwang & Frierson, 2010). Using climate models and observations, poleward MSE transports have been argued to drive a significant fraction of Arctic amplification (Alexeev et al., 2005; Armour et al., 2019; Graversen & Burtu, 2016; Graversen & Wang, 2009; Hwang & Frierson, 2010; Kapsch et al., 2013; Skific & Francis, 2013).

The purpose of this study is to further examine how MSE transports have changed in recent decades using observation-based reanalysis data. We examine the years 1980–2018, a period for which Arctic amplification has occurred (e.g., Gong et al., 2017). We decompose the MSE transport trend into contributions from latent energy transport, dry static energy transport and further decompose these transport trends into contributions from anomalies in the circulation and anomalies in the MSE fields. Our aim is to determine if poleward trends in MSE transports are detectable in reanalysis data over recent decades, whether MSE transport trends are due to thermodynamic (MSE changes) or dynamical (circulation) changes, and whether the reanalysis MSE transport trends are obeying a flux-gradient relationship.

In Section 2, we describe the data used and the calculations we undertook in order to separate the MSE transport trends into various contributions from eddies and the overturning circulation. In Section 3, we discuss the results and their implications. We conclude in Section 4.

2. Data and Methods

For this study, we utilize four different reanalysis data sets to examine MSE and MSE transport trends: The European Centre for Medium Range Weather Forecasts (ECMWF) Reanalyses, (a) ERA-Interim (Dee et al., 2011) and (b) ERA5 (Hersbach et al., 2020), (c) the Japanese 55-year Reanalysis (JRA-55; Kobayashi et al., 2015) and (d) the Modern-Era Retrospective Analysis for Research and Applications, version 2 (MERRA2; Gelaro et al., 2017). All reanalysis data sets are examined using 1.25° horizontal resolution except ERA-Interim, for which 2.5° resolution is used. In addition, we used 37 vertical pressure levels for all reanalysis data sets except MERRA2, which provides 42 vertical pressure levels. (The results are not sensitive to the vertical or horizontal resolutions; downloading vertically integrated energy transports directly from ERA-Interim and ERA5, which incorporates 60 and 137 vertical hybrid-sigma pressure levels respectively, leads to nearly identical MSE transport trends even when ERA-Interim is downloaded at 0.75° horizontal resolution).

Using these four reanalyses, the MSE, denoted by $m = L_v q + c_p T + \phi$, and the MSE transport, denoted by $F(\theta, t)$, are computed using the six-hourly specific humidity (q), temperature (T), geopotential (ϕ), surface pressure (p_s) and meridional wind (v) fields:

$$F(\theta, t) = \frac{2\pi a \cos\theta}{g} \left[\int_0^{p_s} v m \, dp \right] \tag{1}$$

where L_v signifies the latent heat of vaporization, c_p the specific heat capacity of dry air at constant pressure, a the Earth's radius, θ latitude, t time, g gravity, and p pressure. The brackets denote a zonal mean and for conciseness, we will hereafter denote the quantity $\frac{2\pi a \cos\theta}{g}$ as $C(\theta)$.

In practice, the vertical integral in Equation 1 is discretized by computing dp as a centered difference at each pressure level i, where $i = 0$ at the topmost level, such that $dp \approx \Delta p_i = (p_{i+1} - p_{i-1})/2.0$, except at the lowest pressure level above the surface where $dp \approx \Delta p_i = p_s - (p_i + p_{i-1})/2.0$ and at the top of the atmosphere where $dp \approx \Delta p_0 = (p_0 + p_1)/2.0$. Pressure levels below the surface have $dp = 0.0$ and are therefore excluded from the vertical integral (To compute the vertical integral and the pressure weights, we utilized NCAR command language routines dpres_plevel and wgt_vertical_n).

The resulting climatological, that is, time average, vertically integrated MSE (red line) and MSE transport (Equation 1; blue line) are shown for each reanalysis in Figure 1 (left column), for which reasonable agreement can be seen between ERA-Interim, ERA5 and JRA-55. MERRA2, on the other hand, shows climatological MSE transports that are about 20% stronger than any of the other reanalysis products in the extratropics. As will be discussed further, we urge the reader to limit their physical interpretation of reanalysis trends in MSE transport, and this urge is particularly strong for MERRA2, given the likely climatological bias.

The trends in MSE and MSE transport are computed from 1980 to 2018 (Figure 1; right column), for which all of the reanalysis MSE transport trends disagree considerably, as will be examined further in Section 3. To determine the relative contributions to the MSE transport trend by the circulation and MSE fields, we divide the MSE transport (Equation 1) into components by letting $v = \overline{v} + v'$, $m = \overline{m} + m'$, and

$$F(\theta,t)/C(\theta) = \left[\int_0^{p_s} \overline{v}\overline{m}' \, dp \right] + \left[\int_0^{p_s} v'\overline{m} dp \right] + \left[\int_0^{p_s} v' m' \, dp \right] + \left[\int_0^{p_s} \overline{v}\overline{m} dp \right] \tag{2}$$

where overbars denote a time mean, primes denote anomalies and we have moved $C(\theta)$ to the left-hand-side (temporarily) solely for the sake of clarity. The time means and anomalies are further subdivided into zonal means and deviations from zonal means,

$$\overline{v} = [\overline{v}] + \overline{v}^* \tag{3}$$

$$v' = [v'] + v'^* \tag{4}$$

$$\overline{m} = [\overline{m}] + \overline{m}^* \tag{5}$$

$$m' = [m'] + m'^* \tag{6}$$

where asterisks superscripting m and v denote the deviation from the zonal mean. (Note that zonal means for Equations 3–6 exclude values beneath the surface.) Utilizing Equations 3–6, the terms on the right-hand-side of Equation 2 are then written as,

$$\left[\int_0^{p_s} \overline{v}\overline{m}' \, dp \right] \approx \left[\int_0^{p_s} [\overline{v}] [m'] \, dp \right] + \left[\int_0^{p_s} \overline{v}^* m'^* dp \right] \tag{7}$$

$$\left[\int_0^{p_s} v'\overline{m} dp \right] \approx \left[\int_0^{p_s} [v'] [\overline{m}] \, dp \right] + \left[\int_0^{p_s} v'^* \overline{m}^* dp \right] \tag{8}$$

$$\left[\int_0^{p_s} v' m' \, dp \right] \approx \left[\int_0^{p_s} [v'] [m'] \, dp \right] + \left[\int_0^{p_s} v'^* m'^* dp \right] \tag{9}$$

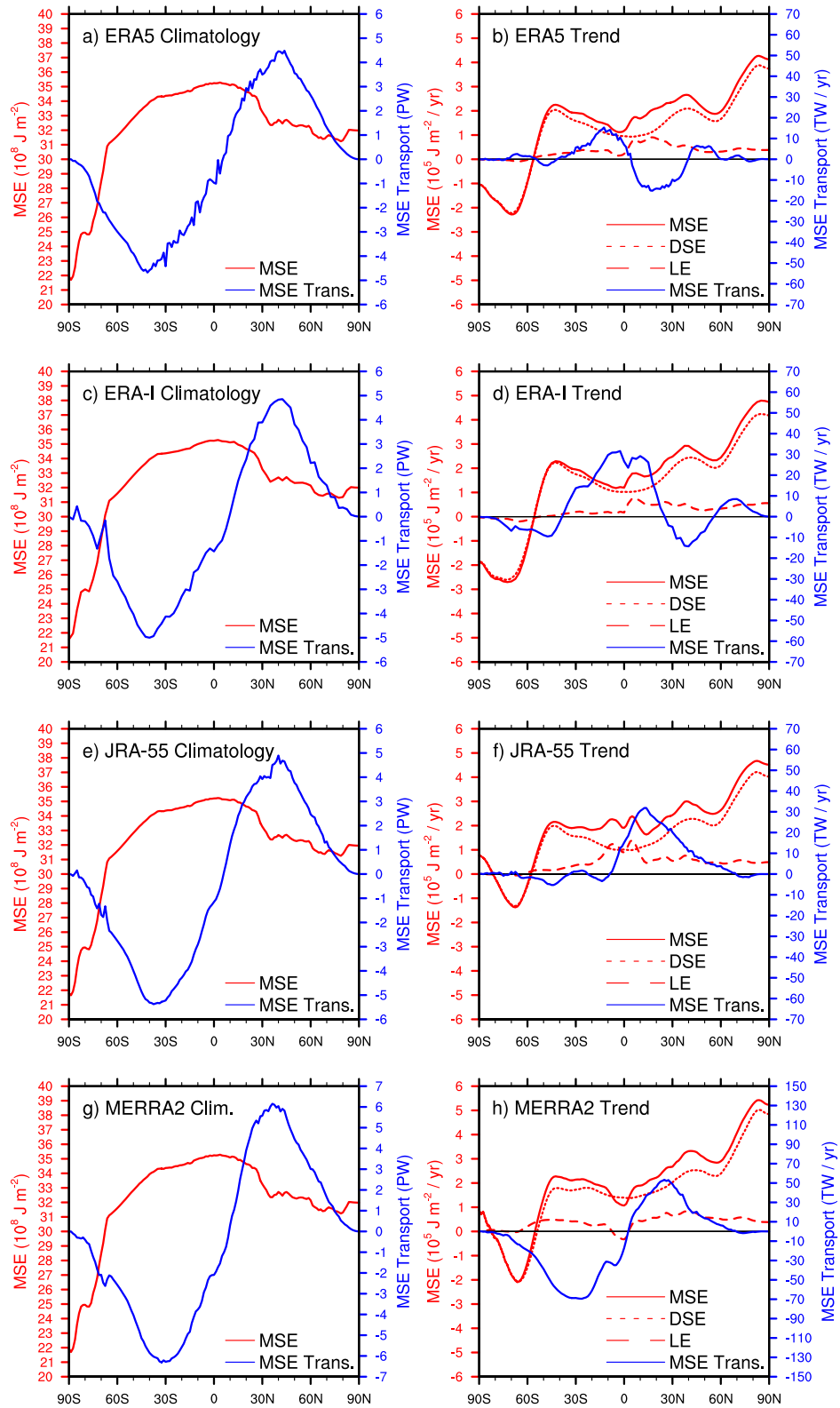

Figure 1. Climatologies (left) and trends (right) in moist static energy (red) and moist static energy transport (blue). In the right panels, the dashed and dotted red lines, respectively, correspond to trends in the latent and dry static energy. Note that there are different right *y*-axes in panels g and h for the Modern-Era Retrospective Analysis for Research and Applications, version 2.

$$\left[\int_0^{p_s} \bar{v}\bar{m}dp\right] \approx \left[\int_0^{p_s} [\overline{v}]\,[\overline{m}]\,dp\right] + \left[\int_0^{p_s} \overline{v}^*\overline{m}^*dp\right] \tag{10}$$

where we neglected terms of the form $\left[\int_0^{p_s}[v]m^*dp\right]$ and $\left[\int_0^{p_s} v^*[m]dp\right]$ since the only contribution to their zonal means would be from the zonal covariance between m^* or v^* with the surface pressure, p_s. Neglecting these terms leads to a small residual.

It is interesting to note that the two terms on the right-hand-side of Equation 10 include the mean meridional overturning circulation $[\overline{v}]\,[\overline{m}]$ and the stationary eddy $\overline{v}^*\overline{m}^*$ contributions to the time mean MSE transport (e.g., Hartmann, 2016; Peixoto & Oort, 1992). In addition, the time average of Equation 9 would result in the transient eddy $\overline{v'^*m'^*}$ and transient overturning circulation $\overline{[v'][m']}$ contributions to the time mean MSE transport (e.g., Hartmann, 2016; Peixoto & Oort, 1992). In a time-average analysis, Equations 7 and 8 will vanish while Equation 9 and 10 remain. However, in an analysis of trends, Equations 7–9 remain while Equation 10 vanishes because Equation 10 is time independent.

The terms on the right-hand-side of Equations 7 and 8 can be interpreted as follows; $\overline{v}^*m'^*$ and $v'^*\overline{m}^*$, respectively, represent changes to the eddy MSE transport caused by changes in the eddy MSE field m'^* and the eddy circulation field v'^*. Next, the terms $[\overline{v}]\,[m']$ and $[v']\,[\overline{m}]$ represent changes to the overturning MSE transport caused by changes in the zonal mean MSE field, $[m']$ and the zonal mean meridional wind $[v']$ field, respectively. Finally, it is important to note that the terms on the right-hand-side of Equation 9 also have trends representing the nonlinear interaction between MSE fields and meridional wind fields for both the overturning $[v']\,[m']$ and eddy $v'^*m'^*$ contributions to the MSE transport.

Removing the time independent terms, that is, Equation 10, the trend, Δ, in MSE transport can be decomposed as follows

$$\begin{aligned}{}^{\Delta F(\theta,t)}/_{C(\theta)} \;=\;& \Delta\left[\int_0^{p_s}[\overline{v}]\,[m']\,dp\right] + \Delta\left[\int_0^{p_s}\overline{v}^*m'^*dp\right] + \Delta\left[\int_0^{p_s}[v']\,[\overline{m}]\,dp\right] + \Delta\left[\int_0^{p_s}v'^*\overline{m}^*dp\right] \\ &+ \Delta\left[\int_0^{p_s}[v']\,[m']\,dp\right] + \Delta\left[\int_0^{p_s}v'^*m'^*dp\right]\end{aligned} \tag{11}$$

Therefore, the MSE transport trend has contributions from (a) the anomalous wind acting on the climatological MSE field, $\Delta\left[\int_0^{p_s}[v']\,[\overline{m}]\,dp\right] + \Delta\left[\int_0^{p_s}v'^*\overline{m}^*dp\right]$, (b) the climatological wind acting on the anomalous MSE field, $\Delta\left[\int_0^{p_s}[\overline{v}]\,[m']\,dp\right] + \Delta\left[\int_0^{p_s}\overline{v}^*m'^*dp\right]$, and (c) the anomalous wind acting on the anomalous MSE field, $\Delta\left[\int_0^{p_s}[v']\,[m']\,dp\right] + \Delta\left[\int_0^{p_s}v'^*m'^*dp\right]$. These three contributions themselves have contributions from the zonal mean and eddy (deviation from zonal mean) fields as discussed above. This leads to the six terms in Equation 11, which can be further subdivided into their latent (vL_vq) and dry static ($vc_pT + v\phi$) energy parts.

3. Results

3.1. Trends

As stated in the introduction, century-long CO_2-forced climate model simulations predict an increase in poleward MSE transports with warming, which has been conceptualized using Clausius-Clapeyron scaling and an assumption that externally forced changes in the circulation are negligible (e.g., Held & Soden, 2006). However, except for MERRA2, reanalysis trends from 1980 through 2018 (Figure 1; blue lines in the right columns) do not show widespread poleward MSE transport trends in both hemispheres even though substantial Arctic amplification has occurred. Instead, ERA5 shows equatorward MSE transports between 45°S and 45°N with weakly poleward or negligible MSE transports elsewhere (Figure 1b); ERA-Interim shows a northward MSE transport trend between 50°S and 25°N and poleward of 50°N and southward MSE transport trends everywhere else (Figure 1d); and JRA-55 shows pronounced northward MSE transport trends throughout the Northern Hemisphere (Figure 1f). Although MERRA2 shows poleward transports (Figure 1h), the decomposition of this trend into latent versus dry static parts, and further into dynamical versus thermodynamical parts, is inconsistent with century-long CO_2-forced climate model simulations, as will be discussed further.

Although the signs of the reanalysis trends in MSE transports are inconsistent with century-long CO_2-forced climate model simulations, except for MERRA2, that the MSE transport trends depend on the reanalysis product (Figure 1; right) strongly limits the extent to which the reanalysis trends can be physically interpreted—a finding

that should be considered in future work examining MSE transports with reanalysis data. Due to the reanalysis dependence, we proceed with the centrally important caveat that some of the findings we report are likely to be artifacts of reanalysis data assimilation procedures that should be revisited at a future time when more reliable data become available. In addition, we also proceed with the objective to better understand what causes the reanalysis dependence for MSE transport trends in order to better inform future studies seeking to utilize reanalysis data sets to study variability in MSE transports. As we will show, there are aspects to reanalysis MSE transport trends that are consistent and can lead to insights, even though the direction of total MSE transport trends do differ across reanalysis products.

In Figure 2, we present our analysis of the dynamical (circulation-driven) and thermodynamical (MSE-driven) contributions to the MSE transport trends for ERA5. Figures S1–S3 in Supporting Information S1 show analogous figures for ERA-Interim, JRA-55 and MERRA2. Using the methodology presented in Section 2, the MSE transport trend is split into contributions from eddies, that is, products of zonal asymmetries, and the overturning circulation, that is, products of zonal mean quantities, and then further into contributions from changes in the meridional wind field (blue), MSE field (red) and their nonlinear interaction (green). Finally, rows 2 and 3 of Figure 2 show the individual contributions to the MSE transport trends from the latent and dry static energy transports.

Most of the MSE transport trend in ERA5 is due to changes in the overturning circulation, $\left[\int_0^{p_s}\left[\overline{v}\right]\left[m'\right]dp\right]+\left[\int_0^{p_s}\left[v'\right]\left[\overline{m}\right]dp\right]+\left[\int_0^{p_s}\left[v'\right]\left[m'\right]dp\right]$ (medium gray line), with eddies, $\left[\int_0^{p_s}\overline{v}^{*}m'^{*}dp\right]+\left[\int_0^{p_s}v'^{*}\overline{m}^{*}dp\right]+\left[\int_0^{p_s}v'^{*}m'^{*}dp\right]$ (light gray line) contributing nearly an order of magnitude less to the MSE transport trend than the overturning circulation at latitudes where the MSE transport trend peaks (Figure 2a). Interestingly, Figure 2a shows that eddies contribute to an increase in poleward MSE transport trends at many latitudes, particularly in the Southern Hemisphere, but this increase is small compared to the MSE transport trend attributable to changes in the overturning circulation. Figures S1–S3 in Supporting Information S1 show that the conclusions drawn above for ERA5 hold also for ERA-Interim, JRA-55 and MERRA2.

In Figures 2b and 2c, we turn our attention to the question of whether changes in the MSE field ($\left[\int_0^{p_s}\left[\overline{v}\right]\left[m'\right]dp\right]$ and $\left[\int_0^{p_s}\overline{v}^{*}m'^{*}dp\right]$; red lines), circulation field ($\left[\int_0^{p_s}\left[v'\right]\left[\overline{m}\right]dp\right]$ and $\left[\int_0^{p_s}v'^{*}\overline{m}^{*}dp\right]$; blue lines), or nonlinearities ($\left[\int_0^{p_s}\left[v'\right]\left[m'\right]dp\right]$ and $\left[\int_0^{p_s}v'^{*}m'^{*}dp\right]$; green lines) are responsible for the contributions of the eddy-driven and overturning circulation MSE transport trends. In the case of the eddy-driven MSE transports ($\left[\int_0^{p_s}\overline{v}^{*}m'^{*}dp\right]+\left[\int_0^{p_s}v'^{*}\overline{m}^{*}dp\right]+\left[\int_0^{p_s}v'^{*}m'^{*}dp\right]$; Figure 2b), the MSE field, meridional wind field and nonlinearities all play a role. This holds for all four reanalysis products (Figures S1b, S2b, and S3b in Supporting Information S1). In contrast, MSE transport trends associated with the overturning circulation are explained almost entirely by changes in the zonal mean meridional wind ($\left[\int_0^{p_s}\left[v'\right]\left[\overline{m}\right]dp\right]$; for all four reanalysis products; blue lines in Figures 2c and Figures S1c, S2c, and S3c in Supporting Information S1).

Unlike the trend in the overturning MSE transport, the eddy-driven component of the MSE transport trends are comparable among ERA5, ERA-Interim and JRA-55 (cf. Figure 2, Figures S1 and S2 in Supporting Information S1). Furthermore, we find that the reanalysis disagreement is considerably stronger for the dry static energy transport than for the latent energy transport (Figure S4 in Supporting Information S1)—a consequence of the reanalyses disagreeing on the zonal mean meridional wind trend in mid to upper levels, where latent energy is climatologically small, but dry static energy is climatologically large. That the reanalysis disagreement in the MSE transport trends can be pinpointed to the trends in the zonal mean meridional wind in mid to upper levels can be deduced from Figure S5 in Supporting Information S1, which shows that the reanalyses disagree on the trend in MSE transport considerably more above 850 hPa than below 850 hPa. Recalling (a) that the trend in the meridional wind drives most of the MSE transport (Figure 2 and Figures S1–S3 in Supporting Information S1) and (b) that the MSE climatologically is similar among the reanalyses (Figure 1; red lines in the left column), the reanalysis differences in the mid to upper troposphere in Figure S5 in Supporting Information S1 are a consequence of differences in the trend of the zonal mean meridional wind.

The timeseries of MSE transports, shown in Figure 3, provides additional insight into the trends shown in Figures 1 and 2. Examining Figures 3c, 3f and 3i, 3l, with the exception of MERRA2, we see that the contribution to the anomalous MSE transport by the zonal mean meridional wind is not characterized by short time scale (approximately 1 year) pronounced changes. Rather, the timeseries of anomalous MSE transports due to the zonal mean meridional wind is dominated by slow low frequency changes sustained over decades (Figure 3; leftmost and rightmost columns). In fact, applying a Fourier filter to the timeseries at each latitude, and retaining

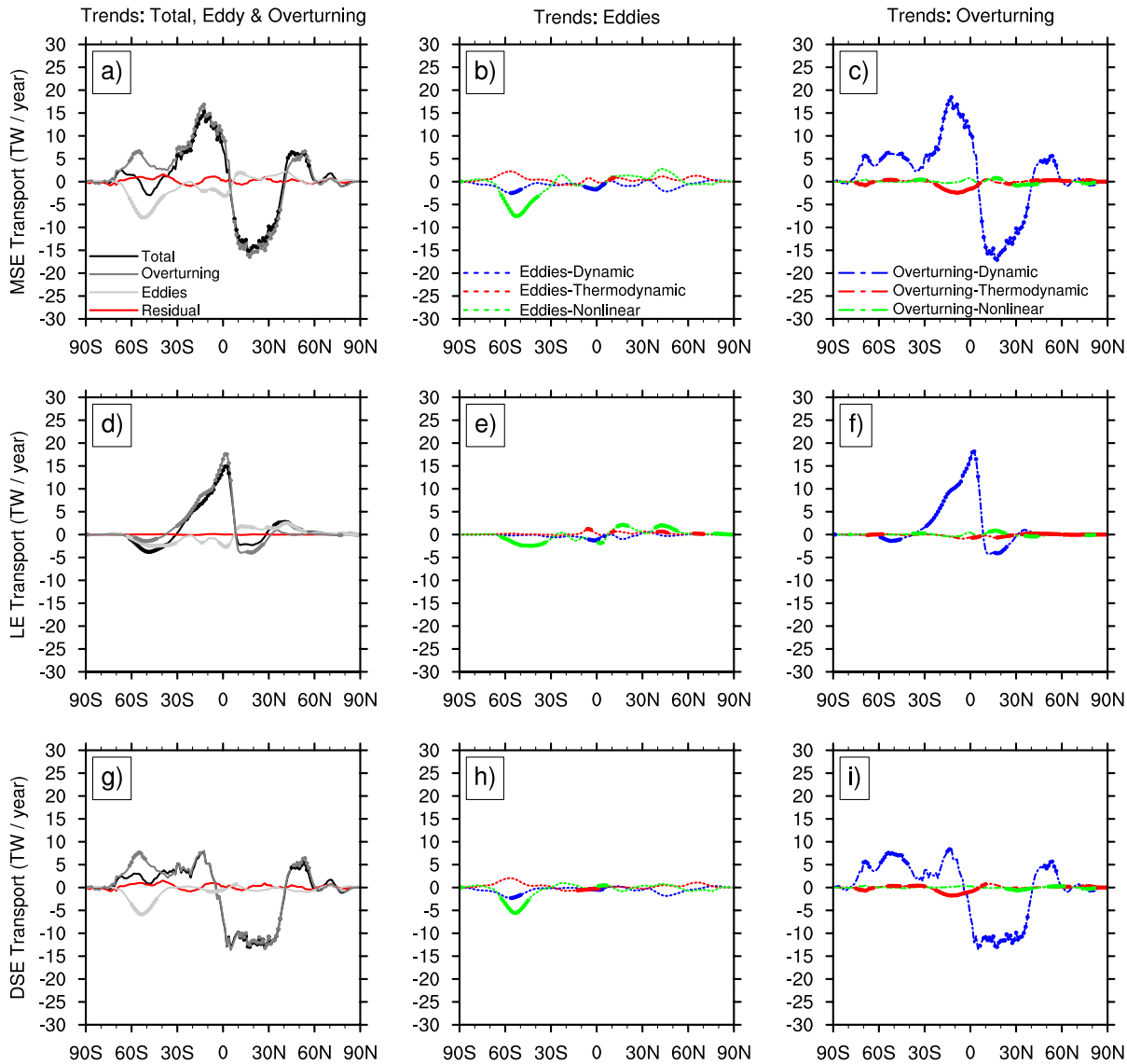

Figure 2. Decomposition of ERA5 northward energy transport trends into parts associated with zonal mean (overturning) anomalies and deviations from zonal mean (eddy) anomalies. The top row corresponds to the moist static energy transport trends, whereas rows two and three, respectively, correspond to the latent energy transport trends and the dry static energy transport trends. The gray shading in the leftmost column splits the energy transport trends into eddy $\left[C(\theta)\int_0^{p_s} v^* m^* dp\right]$ and overturning $\left[C(\theta)\int_0^{p_s}[v][m]dp\right]$ parts, respectively (see Section 2 for details regarding notation). The middle column further splits the eddy energy transport $\left[C(\theta)\int_0^{p_s} v^* m^* dp\right]$ into a part associated with circulation (dynamic) anomalies ($\left[C(\theta)\int_0^{p_s} v'^*\overline{m}^* dp\right]$; blue line), thermodynamic anomalies ($\left[C(\theta)\int_0^{p_s} \overline{v}^* m'^* dp\right]$; red line) and their nonlinear interaction ($\left[C(\theta)\int_0^{p_s} v'^* m'^* dp\right]$; green line). Similarly, the rightmost column further splits the overturning energy transport $\left[C(\theta)\int_0^{p_s}[v][m]dp\right]$into parts associated with circulation anomalies ($\left[C(\theta)\int_0^{p_s}[v']\,[\overline{m}]\,dp\right]$; blue line), thermodynamic anomalies ($\left[C(\theta)\int_0^{p_s}[\overline{v}]\,[m']\,dp\right]$; red line) and their nonlinear interaction ($\left[[C(\theta)\int_0^{p_s}[v']\,[m']\,dp\right]$; green line). There is a small residual in the leftmost column, shown by the red line. Filled circles denote statistical significance at the 95% confidence level.

only three harmonics, does not remove a significant fraction of the trend for ERA5, ERA-Interim and JRA-55 (not shown). This contrasts with the eddy-nonlinear contribution (Figure 3b), which exhibits greater interannual variability, as implied by numerous interannual changes in the sign of the anomaly. Notably, the timeseries of the eddy-nonlinear term is less sensitive to the choice of reanalysis (Figure 3; middle column) while the overturning circulation term (Figure 3; rightmost column) is highly sensitive to the choice of reanalysis.

While the overall picture in Figures 1 and 2 is inconsistent both with the CMIP projections of MSE transports and with the idea that MSE transports are responding to changes in the MSE gradient, there are two reconciling factors that should be prominently reiterated before discussing this feature in greater detail (Section 3.2).

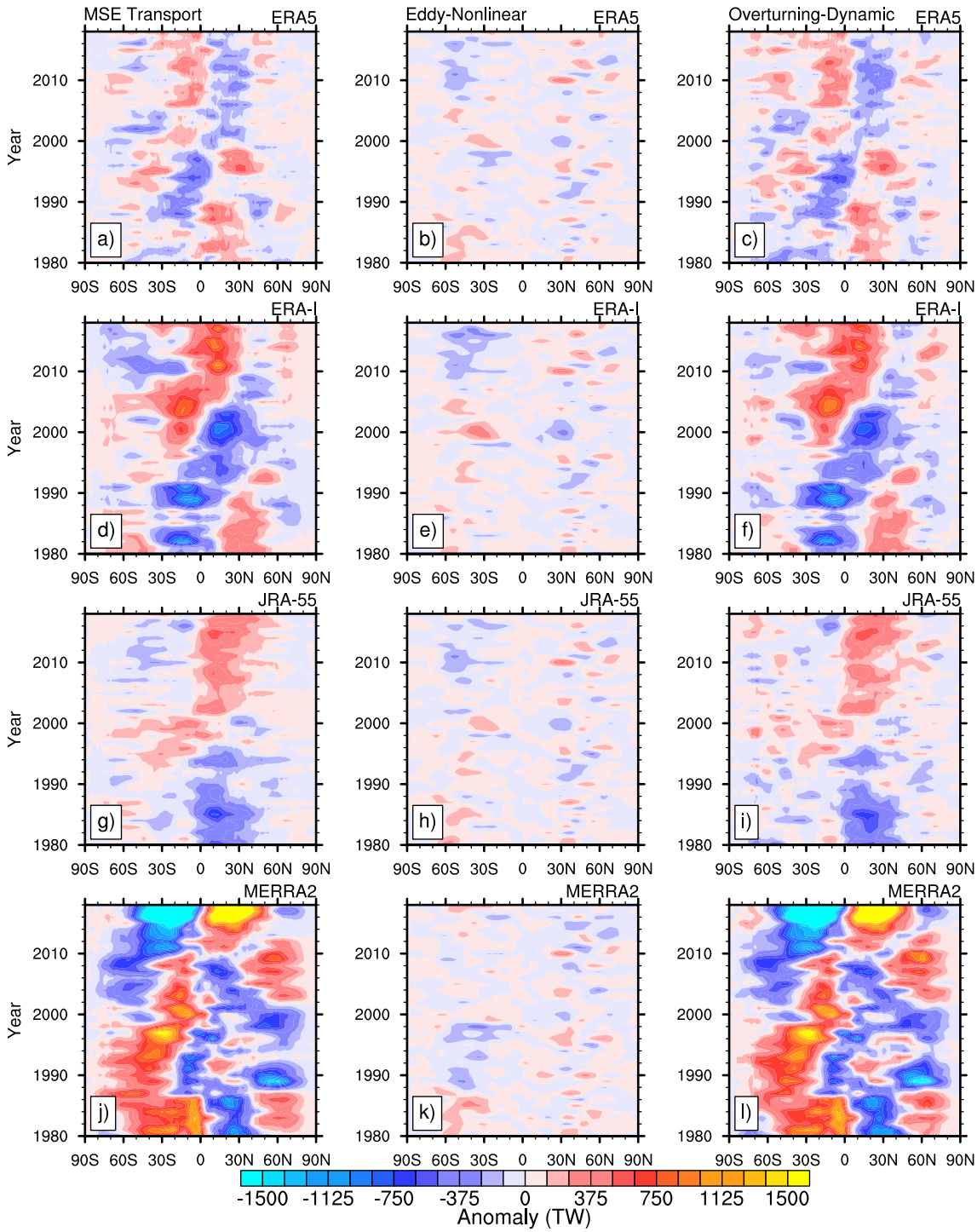

Figure 3. The moist static energy transport anomaly as a function of time (y-axis) and latitude (x-axis). Panels (b and c) respectively show the contribution to the moist static energy transport by nonlinear eddies $\left[C(\theta)\int_{p_s}^{0} v'^{*}m'^{*}dp\right]$ and the zonal mean meridional wind $\left[C(\theta)\int_{p_s}^{0}[v'][\overline{m}]\,dp\right]$ (see Section 2 for more detail).

First, that the reanalysis products do not agree on MSE transport trends indicates that it is challenging to provide a physical interpretation of the MSE transport trends. Second, CMIP projections are on a century long timescale and the MSE transport trends analyzed here (over 38 years) contain a fair degree of internal variability that wouldn't be present in CMIP projections. In spite of these differences, reanalysis products do agree on MSE trends (as opposed to MSE transport trends; discussed subsequently), and in light of the fact

that reanalysis products have some basis in observations, we cannot rule out the possibility that models are not correctly simulating the trends in MSE transports.

3.2. Examining the Flux-Gradient Relationship

Having determined that dynamical changes are crucially contributing to reanalysis MSE transport trends between 1980 and 2018, we next examine more closely the question of whether the reanalysis trends in MSE transport are obeying a flux-gradient relationship. Specifically, we examine MSE trends further to ascertain whether there is any detectable relationship between the MSE transport trend and the gradient in the MSE trend.

In Figure 1 (right columns), it is interesting to note that reanalysis products agree that the rate of MSE increase over the Arctic outpaced that in the tropics and subtropics by a factor of approximately 2. Furthermore, reanalysis products ubiquitously show that the increase in latent energy is not larger over the tropics relative to the midlatitudes, as Clausius-Clapeyron scaling may suggest and as is shown for the near surface in CMIP5 (Armour et al., 2019). Instead, Figure 1 (right panels; dashed red lines) indicates that latent energy increases between 1980 and 2018 are comparable between many latitudes in the extratropics and tropics, with dry static energy trends exceeding latent energy trends at all latitudes (except within the deep tropics for JRA-55 only, where the latent energy trends slightly exceed the dry static energy trends).

The flux-gradient relationship would predict a northward MSE transport trend to coincide with a negative slope in the MSE trend and vice versa for a southward MSE transport trend. Comparing the red and blue lines in Figure 1b, the gradient in the MSE trend does not coincide meaningfully with the MSE transport trend. This is even true for MERRA2, which although shows poleward transport trends, these trends are not obeying a flux-gradient relationship, and appear to be related to particularly strong anomalies between 2015 and 2018 (Figure 3).

As stated earlier, Figures 2 and 3 show that the eddy nonlinear terms are more consistent among the reanalysis products, which is possibly because the eddy terms do not rely upon the zonal mean meridional wind, a variable with a trend that evidently depends on the reanalysis data set (as discussed earlier). Because ERA5, ERA-Interim and JRA-55 agree that the pronounced negative peak over the Southern Ocean (around 60°S) is due to eddies (Figure 2; see also Figures S2 and S3 in Supporting Information S1), and because reanalysis agreement for the eddy term is reasonable, this aspect can be physically interpreted more reliably than the MSE transport trends at other latitudes. Poleward eddy MSE transport trends over the Southern Ocean are associated with storm track shifts (Chemke et al., 2022). Interestingly, relative to reanalysis, climate models considerably underestimate eddy MSE transports over the Southern Ocean due to biases in the zonal wind over the Southern Hemisphere storm tracks (Chemke et al., 2022).

While reanalysis trends in MSE transports contain a fair degree of spread, none of the reanalysis products produce MSE transports that are consistent with a flux-gradient relationship. Though we caution that the reanalysis dependence of MSE transport is a strong limitation, and the possible climatological bias in MERRA2 another limitation, the lack of flux-gradient relationships in reanalysis products also raises a possibility that changes in MSE transports are not responding to changes in MSE gradients. Lee and Yoo (2014) discussed an alternative possibility; they show that during Madden-Julian Oscillation episodes, *enhanced equator to pole gradients in top-of-atmosphere (TOA) net radiation are preceded, not followed, by changes in poleward MSE transports.* Similarly, results from Graversen and Burtu (2016; see their Figures 5a, b) suggest that MSE transports by planetary scale waves produce, rather than remove, anomalous MSE gradients. From a flux-gradient perspective, anomalous MSE transports causing rather than responding to anomalous MSE gradients is counterintuitive. However, as discussed in Lee and Yoo (2014), clouds and moisture fields change the net TOA radiation following changes in MSE transports, which can enable the reverse causality. Indeed, clouds are an important source of spread in climate model projections of poleward MSE transport (Donohoe & Battisti, 2012; Hwang & Frierson, 2010; Zelinka & Hartmann, 2012). That clouds remain a source of uncertainty in climate models perhaps warrants a more cautioned employment of the flux-gradient relationship in future studies.

4. Conclusions

In this study, we examined MSE transports with reanalysis data between 1980 and 2018, a period for which substantial Arctic warming occurred, in order to determine (a) whether there are detectable MSE transport trends in the observational records, (b) whether these trends obeyed a flux-gradient relationship and (c) whether the

MSE transport trends could be attributed to changes in the MSE field or changes in the circulation field. Foremostly, we found that reanalysis products do not agree on the direction of the MSE transport trends during this time period due primarily to differences in the trend of the zonal mean meridional wind. A complicated vertical structure in the trend above 850 hPa causes most of the disagreement, thereby making the dry static energy flux a greater source of reanalysis spread in MSE transports than the latent energy flux (since moisture is largest climatologically below 850 hPa). Because the zonal mean meridional wind is the source of reanalysis dependence, eddy MSE fluxes are in reasonable agreement among reanalysis products compared to overturning MSE fluxes.

Whereas climate models project poleward MSE transport trends as a downgradient response to changes in the MSE field, between 1980 and 2018 we found that the MSE transport trend in reanalyses were not poleward or downgradient, but varied widely depending on the choice of reanalysis. That reanalyses do not show poleward MSE transport trends should not necessarily be taken as evidence for any model deficiency given that the reanalyses disagree and also because the 38-year record is considerably shorter than the century-long CO_2 forced climate model simulations.

Interestingly, although the reanalyses do not agree on the direction of MSE transports, there is reasonable agreement in the vertically integrated trends in MSE. The vertically integrated MSE trends are dominated by increases in dry static energy, even in the tropics where climate models suggest latent energy trends should be larger than dry static energy trends (e.g., Armour et al., 2019). Because MSE trends are reasonably consistent among the reanalyses, this finding is limited primarily by the relatively short data record, unlike the MSE transport trends, which are limited by both the short record and reanalysis dependence.

In light of finding that the anomalous zonal mean meridional wind made the most important contribution to the MSE transport trend between 1980 and 2018, we found no clear evidence that reanalysis MSE transport trends are a response to the MSE gradient. Why MSE transports in reanalyses do not follow a flux-gradient relationship deserves greater attention, particularly because reanalysis products are often used as tools to examine whether climate variability in the observed world matches that in climate models. Furthermore, that reanalysis products are often used as tools to examine climate variability in the observed world also highlights the importance of determining why reanalysis products disagree on MSE transport variability. The results shown here therefore caution the use of flux-gradient relationships to explain the broad range of variability in MSE transports and the observed Arctic warming while also strongly cautioning an immediate trust in reanalysis variability of MSE transports. These cautions stand both until we know that model simulations reliably represent observed MSE transport variability and until a greater understanding of observed MSE transport variability is attained.

Data Availability Statement

All reanalysis data used in this study are publicly obtainable. Detailed instructions on how to download ERA5 can be found at: https://confluence.ecmwf.int/display/CKB/How+to+download+ERA5. ERA-Interim data can be obtained from the following archive: https://apps.ecmwf.int/datasets/data/interim-full-daily/levtype=sfc/. JRA-55 data is available at the NCAR-UCAR Research Data Archive: https://rda.ucar.edu/. MERRA2 data used in this study can be obtained at: https://goldsmr5.gesdisc.eosdis.nasa.gov/data/MERRA2/M2I6NPANA.5.12.4/.

Acknowledgments
We thank Peter Langen and two anonymous reviewers for their comments that greatly improved this manuscript. We also thank Mingyu Park for providing the ERA5 and JRA-55 data used in this study. This research benefitted from discussions that included Mingyu Park, Dong Wan Kim, Cory Baggett, Colton Milcarek and Allen Mewhinney. This study was supported by National Science Foundation grants AGS-1822015 and AGS-1948667.

References

Alexeev, V. A., Langen, P. L., & Bates, J. R. (2005). Polar amplification of surface warming on an aquaplanet in "ghost forcing" experiments without sea ice feedbacks. *Climate Dynamics*, *24*(7), 655–666. https://doi.org/10.1007/s00382-005-0018-3

Armour, K. C., Siler, N., Donohoe, A., & Roe, G. H. (2019). Meridional atmospheric heat transport constrained by energetics and mediated by large-scale diffusion. *Journal of Climate*, *32*(12), 3655–3680. https://doi.org/10.1175/jcli-d-18-0563.1

Carissimo, B. C., Oort, A. H., & Vonder Haar, T. H. (1985). Estimating the meridional energy transports in the atmosphere and ocean. *Journal of Physical Oceanography*, *15*(1), 82–91. https://doi.org/10.1175/1520-0485(1985)015<0082:etmeti>2.0.co;2

Chemke, R., Ming, Y., & Yuval, J. (2022). The intensification of winter mid-latitude storm tracks in the Southern Hemisphere. *Nature Climate Change*, *12*(6), 1–5. https://doi.org/10.1038/s41558-022-01368-8

Dee, D. P., Uppala, S. M., Simmons, A. J., Berrisford, P., Poli, P., Kobayashi, S., et al. (2011). The ERA-Interim reanalysis: Configuration and performance of the data assimilation system. *Quarterly Journal of the Royal Meteorological Society*, *137*(656), 553–597. https://doi.org/10.1002/qj.828

Donohoe, A., & Battisti, D. S. (2012). What determines meridional heat transport in climate models? *Journal of Climate*, *25*(11), 3832–3850. https://doi.org/10.1175/jcli-d-11-00257.1

Gelaro, R., McCarty, W., Suarez, M. J., Todling, R., Molod, A., Takacs, L., et al. (2017). The modern-era retrospective analysis for research and applications, version 2 (MERRA-2). *Journal of Climate*, *30*(14), 5419–5454. https://doi.org/10.1175/JCLI-D-16-0758.1

Gong, T., Feldstein, S., & Lee, S. (2017). The role of downward infrared radiation in the recent Arctic winter warming trend. *Journal of Climate*, *30*(13), 4937–4949. https://doi.org/10.1175/jcli-d-16-0180.1

Graversen, R. G., & Burtu, M. (2016). Arctic amplification enhanced by latent energy transport of atmospheric planetary waves. *Quarterly Journal of the Royal Meteorological Society*, *142*(698), 2046–2054. https://doi.org/10.1002/qj.2802

Graversen, R. G., & Wang, M. (2009). Polar amplification in a coupled climate model with locked albedo. *Climate Dynamics*, *33*(5), 629–643. https://doi.org/10.1007/s00382-009-0535-6

Hartmann, D. L. (2016). Atmospheric motions and the meridional transport of energy. In *Global physical climatology* (pp. 159–192). Elsevier.

Held, I. M., & Soden, B. J. (2006). Robust responses of the hydrological cycle to global warming. *Journal of Climate*, *19*(21), 5686–5699. https://doi.org/10.1175/jcli3990.1

Hersbach, H., Bell, B., Berrisford, P., Hirahara, S., Horanyi, A., Munoz-Sabater, J., et al. (2020). The ERA5 global reanalysis. *Quarterly Journal of the Royal Meteorological Society*, *146*(730), 1999–2049. https://doi.org/10.1002/qj.3803

Hwang, Y. T., & Frierson, D. M. (2010). Increasing atmospheric poleward energy transport with global warming. *Geophysical Research Letters*, *37*(24). https://doi.org/10.1029/2010gl045440

Hwang, Y. T., Frierson, D. M., & Kay, J. E. (2011). Coupling between Arctic feedbacks and changes in poleward energy transport. *Geophysical Research Letters*, *38*(17). https://doi.org/10.1029/2011gl048546

Kapsch, M. L., Graversen, R. G., & Tjernström, M. (2013). Springtime atmospheric energy transport and the control of Arctic summer sea-ice extent. *Nature Climate Change*, *3*(8), 744–748. https://doi.org/10.1038/nclimate1884

Kobayashi, S., Ota, Y., Harada, Y., Ebita, A., Moriya, M., Onoda, H., et al. (2015). The JRA-55 reanalysis: General specifications and basic characteristics. *Journal of the Meteorological Society of Japan. Ser. II*, *93*(1), 5–48. https://doi.org/10.2151/jmsj.2015-001

Lee, S., & Yoo, C. (2014). On the causal relationship between poleward heat flux and the equator-to-pole temperature gradient: A cautionary tale. *Journal of Climate*, *27*(17), 6519–6525. https://doi.org/10.1175/JCLI-D-14-00236.1

Manabe, S., & Wetherald, R. T. (1975). The effects of doubling the CO_2 concentration on the climate of a general circulation model. *Journal of the Atmospheric Sciences*, *32*(1), 3–15. https://doi.org/10.1175/1520-0469(1975)032<0003:TEODTC>2.0.CO;2

Peixoto, & Oort (1992). Energetics. *Physics of Climate*, 308–364.

Skific, N., & Francis, J. A. (2013). Drivers of projected change in Arctic moist static energy transport. *Journal of Geophysical Research: Atmospheres*, *118*(7), 2748–2761. https://doi.org/10.1002/jgrd.50292

Zelinka, M. D., & Hartmann, D. L. (2012). Climate feedbacks and their implications for poleward energy flux changes in a warming climate. *Journal of Climate*, *25*(2), 608–624. https://doi.org/10.1175/JCLI-D-11-00096.1